Available online at www.sciencedirect.com
ScienceDirect
Catalysis Today 117 (2006) 15–21
CATALYSIS TODAY
www.elsevier.com/locate/cattod

Bio-inspired nonheme iron catalysts for olefin oxidation

Paul D. Oldenburg, Lawrence Que Jr.*

Department of Chemistry and Center for Metals in Biocatalysis, University of Minnesota, Minneapolis, MN 55455, USA

Available online 19 June 2006

Abstract

A number of nonheme iron complexes have recently been identified that catalyze the epoxidation and *cis*-dihydroxylation of olefins with H_2O_2 as oxidant. These catalysts have been inspired by a class of arene-dihydroxylating enzymes called the Rieske dioxygenases, the active sites of which consist of an iron center ligated by two histidines and a bidentate aspartate residue. The two remaining sites are *cis* to each other and utilized for oxygen activation. The most effective biomimetic catalysts thus far have polydentate ligands that provide two such *cis*-oriented labile sites to activate the H_2O_2 oxidant. This overview summarizes recent developments in this sub-field of bio-inspired oxidation catalysis and discusses the evolution of the mechanistic pathways proposed to rationalize the new experimental results and the dichotomy between olefin epoxidation versus *cis*-dihydroxylation.

Keywords: Nonheme iron; Biomimetic; Epoxidation; *cis*-Dihydroxylation; H_2O_2

1. Introduction

A family of bio-inspired nonheme iron catalysts has been discovered in the past few years that oxidize olefins efficiently using H_2O_2 as oxidant [1]. These complexes differ from previously reported iron catalysts in their ability to catalyze olefin *cis*-dihydroxylation, representing the first examples by a non-biological iron center. *cis*-Dihydroxylation in nature is carried out by Rieske dioxygenases, which are nonheme iron enzymes that convert arenes into *cis*-dihydrodiol derivatives in the first step of arene biodegradation by soil bacteria [2]. The active sites of these enzymes consist of an iron center ligated to two histidines and a bidentate aspartate [3] (Fig. 1) in a variation of the emerging 2-His-1-carboxylate facial triad motif common to many oxygen activating mononuclear nonheme iron enzymes [4]. This arrangement of ligands results in the availability of two *cis* labile sites that may be used for the activation of dioxygen. Indeed the structure of the enzyme–substrate–O_2 adduct of naphthalene dioxygenase features a side-on bound dioxygen moiety that is poised to attack the target double bond on the substrate (Fig. 1) [5]. The bio-inspired catalysts consist mainly of iron complexes with tetradentate N4 ligands that provide, like enzyme active sites, two *cis*-labile sites at which the H_2O_2 oxidant can be efficiently activated (Fig. 2). Overall, the data accumulated over the last few years (Table 1) reveal a surprisingly complex reaction landscape on which olefin epoxidation is favored under some conditions and *cis*-dihydroxylation under others, suggesting that these two reactions are in fact closely related [6,7].

2. Structure–reactivity correlation

Fig. 2 shows the structures of two prototypical catalysts, Fe(BPMEN) (**1**) and Fe(TPA) (**2**), derived, respectively, from a linear and a tripodal tetradentate ligand. Variations of these motifs can be found embodied in many ligands that have been tested in recent years (Fig. 3) for their effectivity in iron-catalyzed oxidation of olefins. While tripodal ligands invariably give rise to metal centers with *cis* labile sites that are *trans* to different ligating groups, their linear counterparts can adopt two possible coordination topologies where the labile sites are *cis*:*cis*-α where the labile sites are both *trans* to tertiary amine ligands and are thus equivalent, and *cis*-β, where the labile sites are *trans* to different ligating groups like the tripodal ligands (Fig. 4). A third possible topology designated *trans* is one with the four ligating atoms occupying the equatorial plane and with the labile sites *trans* to each other (Fig. 4); this topology is not adopted by the linear N4 ligands discussed here but is represented in Table 1 by the macrocylic cyclam ligated complex, Fe(cyclam) (**C**).

* Corresponding author. Tel.: +1 612 625 0389; fax: +1 612 624 7029.
E-mail address: que@chem.umn.edu (L. Que Jr.).

0920-5861/$ – see front matter
doi:10.1016/j.cattod.2006.05.022

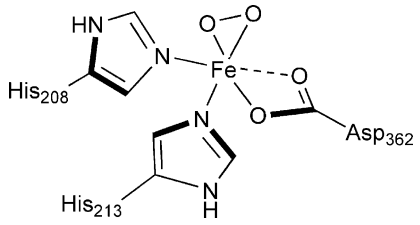

Fig. 1. Structure of the monoiron active site of naphthalene 1,2-dioxygenase with side-on bound dioxygen (1O7N pdb).

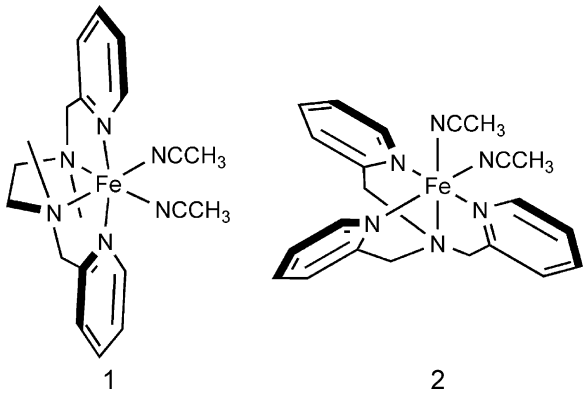

Fig. 2. The first examples of nonheme iron catalysts capable of olefin epoxidation and *cis*-dihydroxylation.

Table 1
Oxidation of cyclooctene with H_2O_2 catalyzed by nonheme iron complexes in CH_3CN

	Maximum TON[a]	Epoxide[b]	Diol[b]	H_2O_2 conv[c] (%)	Reference
1	10	7.5	0.9	84	[6]
2	10	3.4	4.0	74	[6]
α-**3**	10	5.9	0.6	65	[8]
β-**3**	10	2.7	5.0	77	[8]
4	50	14	23	74	[9]
5	10	0.4	6.7	71	[6]
6	10	1.5	6.4	79	[10]
7	20	5.4	11.2	83	[10]
8	300	40	6	15	[11]
9	35	5.7		16	[12]
10a	10	0		0	[13]
10b	10	0.6		6	[13]
10c	10	3.1		31	[13]
11	10	0.5	7.0	75	[14]
12[d]	34	7	23	87[e]	[15]
C[f]	50	20		40	[16]

[a] Indicates the maximum catalytic turnover where the limiting reagent is H_2O_2.
[b] Yields expressed as turnover number (TON), equaling moles of product per mole of iron.
[c] The percent of H_2O_2 converted into epoxide and diol products.
[d] Substrate = 1-octene.
[e] Limiting reagent is substrate, therefore this value corresponds to the percent of substrate converted to product.
[f] C = $[Fe^{II}(cyclam)]^{2+}$, substrate = cyclohexene.

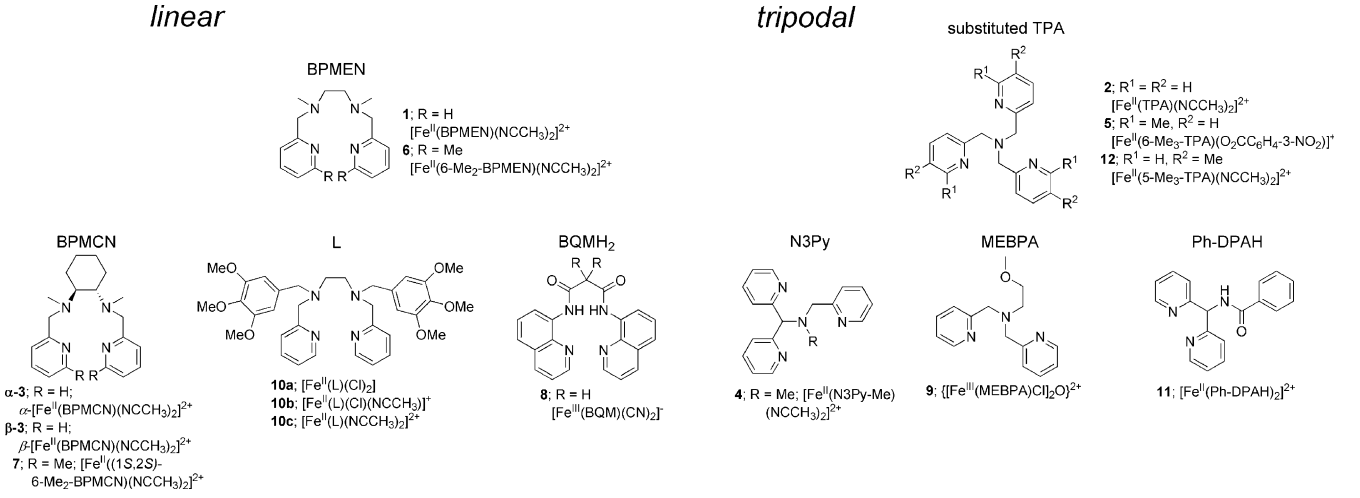

Fig. 3. The ligands and their respective iron complexes discussed herein.

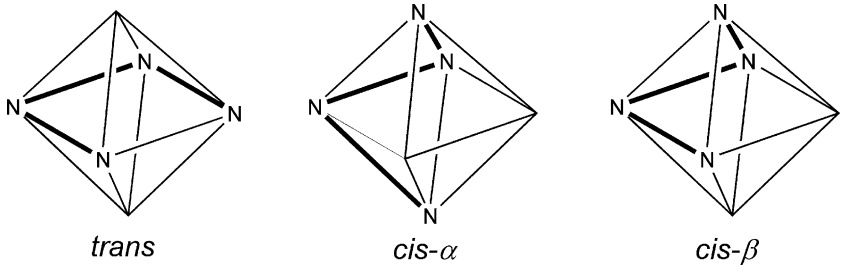

Fig. 4. Possible coordination topologies for linear, tetradentate ligands.

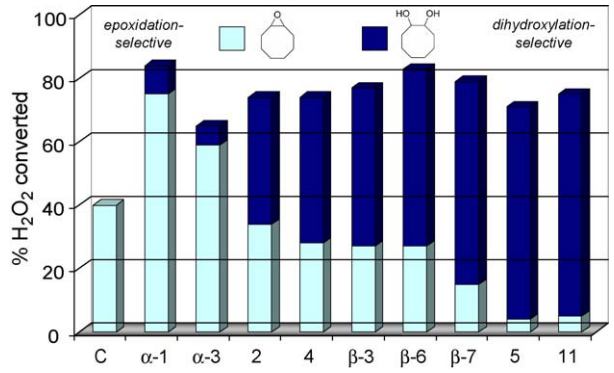

Fig. 5. Percent of H_2O_2 converted into epoxide and *cis*-diol products from cyclooctene substrate catalyzed by nonheme iron complexes.

Fig. 5 compares the reactivity of the more effective catalysts in olefin oxidation with cyclooctene as substrate and 10 equivalents of H_2O_2 as oxidant [8–10,14,16,17]. The conversion efficiency of oxidant to olefin oxidation products can be as high as 84%, and diol-to-epoxide ratios range from <0.1:1 to 14:1. It is clear that the diol does not derive from the epoxide, as both products are observed to form at the same time and the diol-to-epoxide ratio associated with a particular catalyst changes only slightly as the number of turnovers increases. Furthermore, the use of epoxide as a potential substrate under the same reaction conditions does not afford *cis*-diol.

The complexes arrayed in Fig. 5 exhibit a range of olefin oxidation activity, which categorizes them into four types. The first type, represented by C, contains a ligand that adopts a *trans* topology and yields only epoxide as product [16]. The second type is highly selective for epoxide formation and consists of α-**1** and α-**3**, which have ligands that adopt a *cis*-α topology [6,8]. The *cis*-α topology gives rise to equivalent labile sites, both being *trans* to an amine function. The next type consists of **2**, β-**3**, and **4**, which favor diol formation but still produce a significant amount of epoxide (1:1 < diol-to-epoxide ratio < 2:1) [6,8,9]. These complexes have inequivalent labile sites that are, respectively, *trans* to an amine and a pyridine ligand. The last type is highly diol selective (diol-to-epoxide ratios > 2:1); the labile sites on these complexes (**5**, β-**6**, and β-**7**) are inequivalent like those of the third type and the pyridine ligands all have 6-methyl substituents [6,10]. Thus, the ligand structure appears to exert significant control on the diol-to-epoxide ratio.

3. Oxidation mechanisms

3.1. The water-assisted mechanism

Insights into the mechanisms of these reactions have been obtained from a series of ^{18}O labeling experiments using either $H_2{}^{18}O$ or $H_2{}^{18}O_2$ [6,8,9,14,18]. Since the latter is available commercially only as a 2% aqueous solution, the corresponding $H_2{}^{18}O$ experiment must be carried out by the addition of 1000 equivalents of $H_2{}^{18}O$ in the presence of $H_2{}^{16}O_2$ to achieve complementarity of conditions. The most readily interpretable labeling results are for the *cis*-diol product of **2** [6], where one

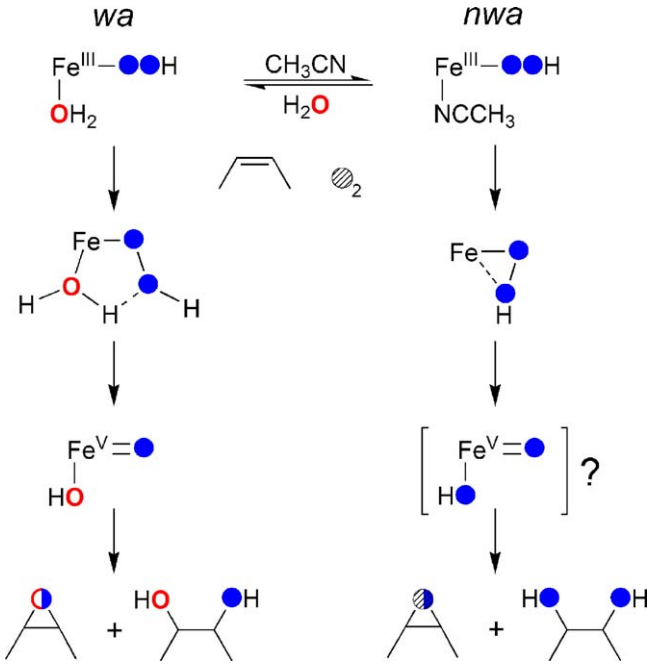

Fig. 6. Proposed mechanisms for iron-catalyzed olefin oxidation. A high-valent iron active species, derived from either a water-assisted (wa) or non-water-assisted (nwa) pathway, has been proposed to be responsible for oxygen atom transfer to susbtrate. Sources of oxygen atoms are H_2O_2 (blue filled circle), H_2O (red unfilled circle), or O_2 (dashed circle) as determined by ^{18}O labeling studies. (For interpretation of the references to color in this figure legend, the reader is referred to the web version of this article.)

diol oxygen derives from H_2O_2 and the other derives from H_2O. This result excludes a direct attack of the activated H_2O_2 on the olefin and O–O bond cleavage must first occur to produce an oxidant that carries out the *cis*-dihydroxylation.

The intriguing labeling results for the diol products of **2** have led to the proposal of a HO–Fe^V=O oxidant derived from an Fe^{III}–OOH intermediate that has been observed in MeCN at −40 °C (Fig. 6, left branch) [6]. The Fe^{III}–OOH intermediate is characterized as having a low-spin iron(III) center that weakens and activates the O–O bond [19]. Water coordinates to the iron(III) center at a site *cis* to the hydroperoxide and hydrogen bonds to the terminal oxygen atom of the hydroperoxide. In this water-assisted (wa) mechanism, the low-spin iron(III) center and the coordinated water act in concert to promote the heterolytic cleavage of the O–O bond to afford the proposed HO–Fe^V=O oxidant. Such a species resembles the *cis*-dioxo high-valent metal centers found in reagents such as MnO_4^- and OsO_4 known to carry out olefin *cis*-dihydroxylation [20,21].

Epoxidation by **2** can also be understood by invoking this same oxidant produced by the wa mechanism. Labeling studies show 8% incorporation of $H_2{}^{18}O$ into the epoxide oxygen [6], which requires that O–O bond cleavage occurs prior to the attack of substrate at least some of the time. The low level of ^{18}O incorporation compared to what is observed for the diol product may be rationalized by the following mechanistic requirements: (a) that epoxidation results only from oxo (but not hydroxo) transfer to the olefin and (b) that oxo-hydroxo tautomerization occurs only to a limited extent before transfer occurs. The latter is not unreasonable considering that the oxo

and hydroxo ligands on the HO–Fe^{V}=O oxidant for TPA have different *trans* ligands and are thus not in equivalent coordination sites, so one isomer is likely to be favored over the other. The generality of the wa mechanism has been established by parallel labeling studies on other catalysts, namely α-**1**, α-**3**, and **4**, that demonstrate label incorporation from H_2O into both epoxide and diol products [8,9,18].

DFT calculations support the viability of the wa mechanism (Fig. 6, left branch) [22]. The postulated conversion of the spectroscopically characterized low-spin Fe^{III}–OOH species resulting from **2** into the HO–Fe^{V}=O oxidant has been found to be energetically quite feasible. This conversion has a calculated barrier of 19.2 kcal mol^{-1}, and the resultant HO–Fe^{V}=O species is only 5.1 kcal mol^{-1} above the reactant (Fig. 7). For this complex, the Fe^{V} oxidation state is attained, rather than being delocalized between metal center and ligand as is the case for the analogous $[(Por^{\bullet})Fe^{IV}{=}O]^{+}$ intermediate associated with heme enzymes [23].

The question of olefin epoxidation and *cis*-dihydroxylation by a common HO–Fe^{V}=O oxidant as implied by the experimental data has also been addressed by DFT calculations [7]. These calculations reveal that epoxidation and *cis*-dihydroxylation of *cis*-2-butene are both very exothermic and have comparable activation barriers, with the latter being favored by only about 1.6 kcal mol^{-1} (Fig. 7). The determining factor between the epoxidation and *cis*-dihydroxylation pathways stems from which oxygen of the active species initiates olefin attack. Epoxidation occurs by oxo attack on the olefin, while *cis*-dihydroxylation is initiated by hydroxo attack. Experiments should be devised to test this particularly important mechanistic insight, obtainable thus far only by computation.

3.2. The non-water-assisted mechanism

Labeling experiments also provide evidence for a non-water-assisted (nwa) mechanism that applies to the more diol-selective catalysts (Fig. 6, right branch). For β-**3** and **5**, both oxygen atoms observed in their *cis*-diol products derive from H_2O_2 [6,8]. Furthermore in the case of **5**, the use of 50:50 $H_2{}^{16}O_2$:$H_2{}^{18}O_2$ does not yield any singly labeled diol product, demonstrating that diol is formed from a single molecule of H_2O_2 [6]. The nwa mechanism is proposed to consist of the initial formation of an Fe^{III}-η^2-OOH intermediate, as in the Rieske dioxygenases, that either cleaves to form a HO–Fe^{V}=O oxidant or attacks the double bond directly. The more diol-

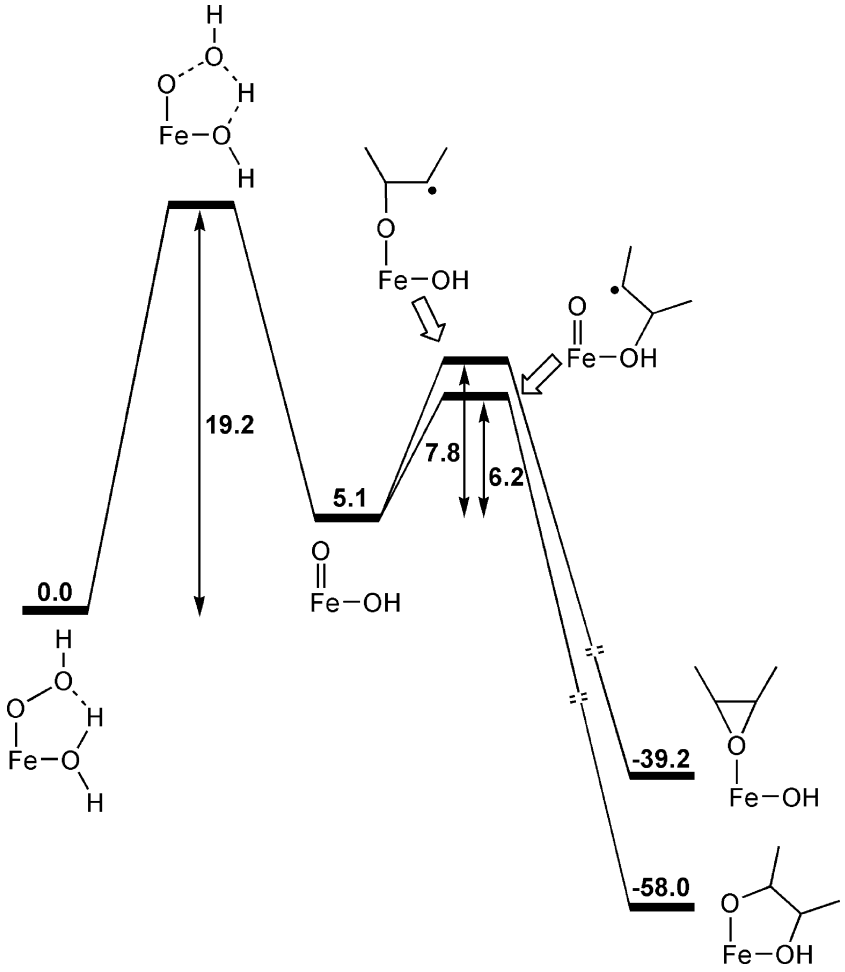

Fig. 7. Reaction pathway for the formation of the HO–Fe^{V}=O intermediate from **2** and its subsequent reaction with 2-butene. The displayed values correspond to free energy with units of kcal mol^{-1}.

selective catalysts tend to have α-methyl pyridine ligands that favor a high-spin iron center, and this spin-state preference may play a role in the choice between wa and nwa pathways [10]. The labeling results are the only evidence thus far supporting the nwa mechanism since no intermediate has been observed for these diol-selective systems, so other mechanistic possibilities should be considered.

4. A *cis*-dihydroxylation-specific nonheme iron catalyst

Very recently, a new iron oxidation catalyst, **11**, with high oxidative efficiency and diol selectivity was reported [14]. This complex differs from the others developed thus far in utilizing a tridentate ligand (Ph-DPAH) (Fig. 3) to provide a facial array of two pyridines and one carbonyl oxygen donor groups that resembles the 2-His-1-carboxylate active site found for the Rieske dioxygenases. The reactivity of **11** closely parallels that associated with the highly diol-selective group of catalysts (type 4 in Fig. 5), which is not surprising since the N,N,O ligand set would be expected to favor a high-spin metal center. ^{18}O-labeling studies reveal that the majority of diol product (64%) contains both oxygen atoms derived exclusively from H_2O_2. However, there is an appreciable amount of diol (33%) with an oxygen atom derived from H_2O and the other from H_2O_2. This labeling result can be rationalized by the presence of a third labile site not available for complexes of tetradentate ligands. Thus for **11**, two of the labile sites can be occupied by a side-on bound peroxide and the third by water (Fig. 8). The fact that water is incorporated into the diol product strongly argues against a concerted attack of the side-on bound peroxo on the target double bond and minimally requires that O–O bond cleavage occurs before the second C–O bond is formed. We favor initial formation of an $(H_2O)HO–Fe^{V}=O$ species that can rearrange to form an $Fe^{V}(OH)_3$ oxidant before attack of substrate.

5. Electrophilic versus nucleophilic oxidants

The dichotomy between epoxide-selective and diol-selective catalysts has led us to investigate the differences that may exist between the oxidizing species produced by the various catalysts of each type. Competition experiments were carried out with pairs of substrates to assess whether the catalyst in question showed a preference for oxidizing electron-rich or electron-poor olefins [24]. The two catalysts chosen for this study were **2**

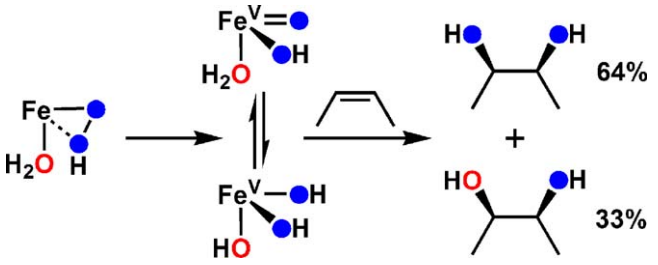

Fig. 8. Proposed mechanism for water incorporation in the *cis*-dihydroxylation of olefins by **11**. Sources of oxygen atoms are H_2O_2 (blue filled circle) or H_2O (red unfilled circle).

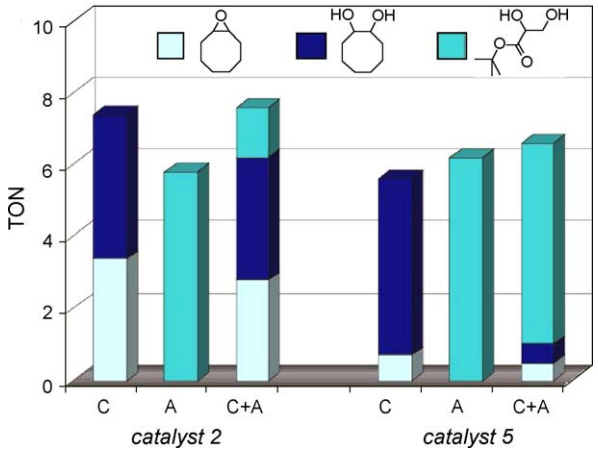

Fig. 9. Product yields resulting from the oxidations of cyclooctene (C), *tert*-butyl acrylate (A), and an equimolar mixture of cyclooctene and *tert*-butyl acrylate (C + A) catalyzed by **2** or **5** with 10 equivalents of H_2O_2 as oxidant.

(representing epoxide forming catalysts) and **5** (exemplifying highly diol-selective catalysts). These experiments revealed that **2** shows a clear preference to oxidize the more electron-rich olefins, while **5** preferentially oxidizes electron-poor olefins (Fig. 9). These opposite trends suggest that **2** reacts with H_2O_2 to generate an electrophilic oxidant, while **5** on the other hand forms a nucleophilic oxidant. This disparity in behavior of these two catalysts may stem from the different spin states of the Fe^{III}–OOH intermediate generated in the course of catalysis. The behavior of **2** is fully consistent with the proposed formation of an electrophilic $HO–Fe^{V}=O$ species in the wa mechanism (Fig. 6, left branch). On the other hand, the nucleophilic oxidant derived from **5** is more difficult to conceptualize. This species could be a yet unobserved (but highly likely) high-spin Fe^{III}-η^2-OOH intermediate or the corresponding $HO–Fe^{V}=O$ species in which olefin attack occurs via the bound hydroxide, as suggested by DFT calculations [7]. Further work needs to be done to rationalize these results more fully.

6. Other nonheme iron oxidation catalysts

Other groups have also investigated the use of nonheme iron complexes as catalysts for olefin oxidation (Table 1). As mentioned already, the N3Py complex (**4**) described by Feringa and co-workers is a comparably active catalyst to the ones investigated in the Que laboratory [9]. Two other studies afford iron(III) complexes that are significantly less effective as catalysts. Artaud and co-workers using the linear, tetradentate ligand $BQMH_2$, providing two quinolyl and two amidate ligating groups, have characterized $[Fe^{III}(BQM)(CN)_2]^-$ (**8**), an iron(III) complex of the ligand coordinated in a *cis*-β topology with the two remaining *cis*-oriented sites occupied by cyano groups [11]. H_2O_2 conversion efficiency is only about 15%, but both epoxide and *cis*-diol are obtained as products with a diol-to-epoxide ratio of 0.15:1. In another report, Reedijk and co-workers have reported a derivative of the TPA ligand where one of the pyridylmethyl arms is replaced by a methoxyethyl group, forming the N3O ligand, MEBPA [12]. Combination with an

iron(III) salt results in the isolation of the dinuclear species, $[(Fe^{III}(MEBPA)Cl)_2O]^{2+}$ (**9**), that catalyzes olefin epoxidation with about 16% conversion efficiency. In both cases, we conjecture that the presence of cyano or chloro ligands retard the activation of H_2O_2 by hampering access to the metal center; however, the iron center appears capable of activating H_2O_2 once the oxidant does gain access.

The deleterious effect of chloride ligands on catalysis has been nicely demonstrated by Ménage and co-workers with the use of a BPMEN ligand where the *N*-methyl groups are replaced with trimethoxybenzyl groups (Fig. 3) [13]. They synthesized a series of three iron(II) complexes in which the two remaining coordination sites were occupied by two chloride ions (**10a**), one chloride and one CH_3CN (**10b**), and two CH_3CN molecules (**10c**) and found that the efficacy of the catalyst depended inversely upon the number of ligated chlorides. Complex **10a** is not at all an olefin oxidation catalyst and reacts with H_2O_2 to produce $HO^{\bullet}$ that hydroxylates the phenyl ring of the ligand. Complex **10b** represents an intermediate case where both olefin epoxidation (6–7% conversion efficiency) and ligand oxidation are observed. Complex **10c** in contrast does not effect ligand oxidation at all and does indeed catalyze olefin epoxidation with 30% conversion efficiency. This series thus emphasizes the need for labile ligands on the iron center to allow efficient access of H_2O_2. Such access promotes inner-sphere oxidation of the iron center to generate the high-valent iron-oxo oxidant, instead of $HO^{\bullet}$ that would be formed by outer-sphere oxidation of the iron center.

7. Towards practical applications

7.1. Olefin epoxidation and cis-dihydroxylation with high substrate conversion

Many of the catalytic systems we have discussed in some detail thus far all afford high conversion of oxidant into epoxide and diol products; however, their utility is limited due to the requirement for a large excess in substrate. Towards a more practical synthetic goal, experiments have been carried out under conditions of limiting substrate. Jacobsen and co-workers found that the use of 3 mol % catalyst, complex **1** in this case, in the presence of 10 equivalents of acetic acid (relative to iron) and 1.5 equivalents of H_2O_2 (relative to substrate) affords up to 90% conversion of the olefin into epoxide [25]. No diol is observed. The nature of oxidizing species formed under these conditions is not established and has been the subject of some discussion [26,27]. Ryu et al. investigated the use of the 5-Me-substituted analogue of TPA (**12**) under similar conditions [15]. With 3 mol % catalyst and 4 equivalents of H_2O_2 (relative to substrate) without the addition of acetic acid, between 75 and 87% conversion of a variety of substrates into both *cis*-diol and epoxide products can be obtained. For example, the oxidation of *cis*-2-heptene affords a diol:epoxide ratio of 3:1. These studies suggest that nonheme iron catalysts may yet become useful in synthetic applications as reaction conditions are further refined.

7.2. Asymmetric cis-dihydroxylation

Yet another potential application of these bio-inspired catalysts is in asymmetric dihydroxylation. Towards this end, the optically active 1*S*,2*S*-isomer of $[Fe^{II}(\beta\text{-}6\text{-}Me_2\text{-}BPMCN)(MeCN)_2]^{2+}$ (**6**) was synthesized [10]. This complex was found to catalyze the *cis*-dihydroxylation of *trans*-2-octene and *trans*-2-heptene with ee's of 82 and 79%, respectively. This first example of iron-catalyzed asymmetric *cis*-dihydroxylation demonstrates the tremendous potential of developing other iron-based asymmetric catalysts to be used as alternatives to asymmetric osmium *cis*-dihydroxylation.

8. Concluding remarks

In conclusion, we have summarized the many features that contribute to the oxidative catalysis of olefin substrates by nonheme iron complexes. Ligand topology has been found to affect the inherent oxidative preferences of these species towards either epoxidation or *cis*-dihydroxylation of olefins by manipulation of the labile sites required for inner-sphere activation of the H_2O_2 oxidant. Although not yet synthetically practical, these complexes may pave the way for the development of new catalysts that could serve as an attractive alternative to more expensive and toxic heavy-metal oxidants.

Acknowledgements

This work was supported by the Department of Energy (DOE DE-FG02-03ER15455). We are grateful to Dr. Rubén Mas-Ballesté for discussions during the writing of this review and the design of figures.

References

[1] K. Chen, M. Costas, L. Que Jr., J. Chem. Soc., Dalton Trans. (2002) 672.
[2] M. Costas, M.P. Mehn, M.P. Jensen, L. Que Jr., Chem. Rev. 104 (2004) 939.
[3] B. Kauppi, K. Lee, E. Carredano, R.E. Parales, D.T. Gibson, H. Eklund, S. Ramaswamy, Structure 6 (1998) 571.
[4] K.D. Koehntop, J.P. Emerson, L. Que Jr., J. Biol. Inorg. Chem. 10 (2005) 87.
[5] A. Karlsson, J.V. Parales, R.E. Parales, D.T. Gibson, H. Eklund, S. Ramaswamy, Science 299 (2003) 1039.
[6] K. Chen, M. Costas, J. Kim, A.K. Tipton, L. Que Jr., J. Am. Chem. Soc. 124 (2002) 3026.
[7] A. Bassan, M.R.A. Blomberg, P.E.M. Siegbahn, L. Que Jr., Angew Chem. Int. Ed. 44 (2005) 2939.
[8] M. Costas, L. Que Jr., Angew. Chem. Int. Ed. 41 (2002) 2179.
[9] M. Klopstra, G. Roelfes, R. Hage, R.M. Kellogg, B.L. Feringa, Eur. J. Inorg. Chem. (2004) 846.
[10] M. Costas, A.K. Tipton, K. Chen, D.-H. Jo, L. Que Jr., J. Am. Chem. Soc. 123 (2001) 6722.
[11] O. Rotthaus, S. Le Roy, A. Tomas, K.M. Barkigia, I. Artaud, Inorg. Chim. Acta 357 (2004) 2211.
[12] S. Tanase, C. Foltz, R. de Gelder, R. Hage, E. Bouwman, J. Reedijk, J. Mol. Catal. A 225 (2005) 161.
[13] Y. Mekmouche, S. Ménage, J. Pécaut, C. Lebrun, L. Reilly, V. Schuenemann, A. Trautwein, M. Fontecave, Eur. J. Inorg. Chem. (2004) 3163.
[14] P.D. Oldenburg, A.A. Shteinman, L. Que Jr., J. Am. Chem. Soc. 127 (2005) 15672.

[15] J.Y. Ryu, J. Kim, M. Costas, K. Chen, W. Nam, L. Que Jr., Chem. Commun. (2002) 1288.
[16] W. Nam, R. Ho, J.S. Valentine, J. Am. Chem. Soc. 113 (1991) 7052.
[17] K. Chen, L. Que Jr., Angew. Chem. Int. Ed. 38 (1999) 2227.
[18] D. Quiñonero, K. Morokuma, D.G. Musaev, R. Mas-Ballesté, L. Que Jr., J. Am. Chem. Soc. 127 (2005) 6548.
[19] R.Y.N. Ho, G. Roelfes, B.L. Feringa, L. Que Jr., J. Am. Chem. Soc. 121 (1999) 264.
[20] J. Brinksma, L. Schmieder, G. van Vliet, R. Boaron, R. Hage, D.E. De Vos, P.L. Alsters, B.L. Feringa, Tetrahedron Lett. 43 (2002) 2619.
[21] H.C. Kolb, M.S. VanNieuwenhze, K.B. Sharpless, Chem. Rev. 94 (1994) 2483.
[22] A. Bassan, M.R.A. Blomberg, P.E.M. Siegbahn, L. Que Jr., J. Am. Chem. Soc. 124 (2002) 11056.
[23] J.H. Dawson, Science 240 (1988) 433.
[24] M. Fujita, M. Costas, L. Que Jr., J. Am. Chem. Soc. 125 (2003) 9912.
[25] M.C. White, A.G. Doyle, E.N. Jacobsen, J. Am. Chem. Soc. 123 (2001) 7194.
[26] M. Fujita, L. Que Jr., Adv. Synth. Catal. 346 (2004) 190.
[27] S. Taktak, M. Flook, B.M. Foxman, L. Que Jr., E.V. Rybak-Akimova, Chem. Commun. (2005) 5301.